



IJRASET

International Journal For Research in
Applied Science and Engineering Technology



INTERNATIONAL JOURNAL FOR RESEARCH

IN APPLIED SCIENCE & ENGINEERING TECHNOLOGY

Volume: 12 **Issue:** V **Month of publication:** May 2024

DOI: <https://doi.org/10.22214/ijraset.2024.62531>

www.ijraset.com

Call:  08813907089

E-mail ID: ijraset@gmail.com

Design of Bladeless Thruster for UAV Application

Yuvraj Ratnaparkhi¹, Sohaam Thakur², Mansi Tilekar³, Parth Punde⁴, Tejas Warbhe⁵

Mechanical Engineering, Vishwakarna Institute of Technology, Pune, India

Abstract: Conventional multi-copters rely on multiple propellers to achieve lift, propulsion, and altitude control. However, a new type of thruster has been developed that offers significant safety advantages by eliminating external blades.

This advanced thruster features a vertical inlet duct equipped with an Electric Ducted Fan (EDF), which is paired with a specially designed nozzle ring. The unique design of the nozzle ring, which has an airfoil-like cross-section, creates a pressure differential that, combined with the Coanda effect, generates thrust without the need for externally rotating blades or propellers. This bladeless technology not only enhances safety but also offers a quieter and potentially more efficient alternative to traditional propeller-based systems.

Keywords: Bladeless Thruster, Coanda Effect, Entrained Air, Induced Air

I. INTRODUCTION

The concept of a bladeless thruster system involves a sophisticated design that enhances both safety and efficiency for unmanned aerial vehicles (UAVs). The thruster system is designed with two main components: an Electric Ducted Fan (EDF) or a specially engineered compressor, and a discharge frame. The role of the electronic components is to draw air from the surrounding environment and direct it towards the discharge frame. This frame is strategically positioned to accelerate the airflow that enters it. The design leverages the principles of pressure differences over an airfoil surface, similar to those used in aerodynamics. When the air is sucked in through the EDF, it passes through the nozzle ring of the discharge frame, creating a low-pressure region at one end of the ring. This induced airflow, combined with the accelerated flow through the frame, results in a high-pressure region at the opposite end of the ring. By harnessing these fundamental principles of lift generation, the system effectively creates thrust without the need for external rotating blades. This innovative propulsion system not only enhances the safety and efficiency of UAVs but also represents a cutting-edge, bladeless design that could revolutionize aerial technology.

II. METHODOLOGY

The concept of a bladeless propulsion system, stemming from the innovative design of a bladeless fan, has become a focal point in contemporary research. It comprises two primary components: a ducted fan or compressor and a discharge frame equipped with an inlet. The ducted fan or compressor assumes a central role in this system, responsible for delivering airflow to the discharge frame. This airflow initiation triggers a suction effect termed "induction," which draws surrounding air into the induced flow, a phenomenon referred to as "entrainment." These dynamics, including entrainment, are fundamental to the system's operation and leverage principles governing lift generation. Essential to the propulsion mechanism is the establishment of differential pressure zones across the system's components. This involves inducing a low-pressure environment along the assembly's periphery, with a high-pressure region within its core. These pressure variations are critical for generating thrust. Furthermore, the integration of the Coanda effect enhances the system's aerodynamic efficiency. The Coanda effect, characterized by a fluid jet adhering to nearby surfaces when encountering curvature, optimizes airflow distribution and maximizes thrust generation. Mathematically, the Coanda effect can be represented by the simplified equation:

$$F = \frac{1}{2} \rho Q^2 A \left(\frac{Cl}{Cd} \right)$$

Where:

- F = represents the force generated by the Coanda effect.
- ρ = denotes the density of the fluid.
- Q = signifies the volumetric flow rate of the fluid.
- A = represents the cross-sectional area over which the fluid flows.
- Cl = denotes the lift coefficient, characterizing the lift generated by the fluid.
- Cd = signifies the drag coefficient, representing the resistance encountered by the fluid.

This equation encapsulates the fundamental relationship between the various parameters governing the Coanda effect, offering insights into the forces at play within the bladeless propulsion system.

The versatility of this propulsion concept extends to applications in Unmanned Aerial Vehicles (UAVs), promising advancements in bladeless UAV designs. A vital aspect of its functionality involves deliberate pressure manipulation between the system's inlet and outlet sections to generate thrust, thereby enhancing overall efficiency.

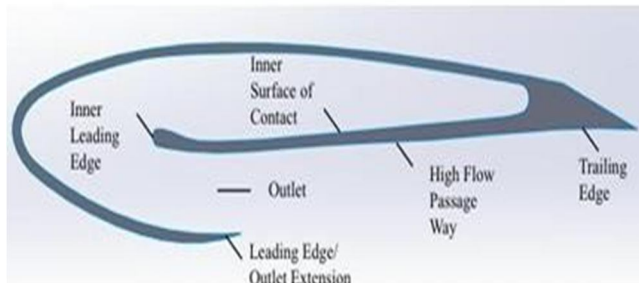


FIG 1. Foil parts (from Anutha M A's Work)

III. DESIGN AND IMPLEMENTATION

A. Design of Thruster ring Cross Section

An airfoil profile, as depicted in FIG 1 and selected from standardized airfoils, was chosen as the cross-section for the thruster due to its pronounced curvature, making it an optimal Coanda surface. This design choice facilitates enhanced suction of air from the rear portion of the discharge ring, crucial for maximizing thruster performance. The airfoil-like cross-section of the nozzle plays a pivotal role in improving thruster efficiency, with

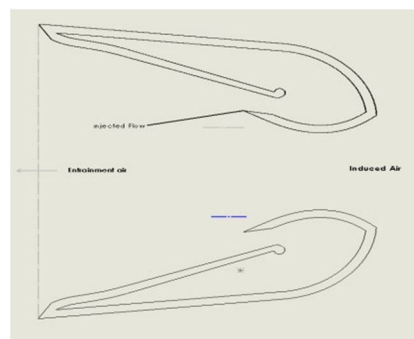
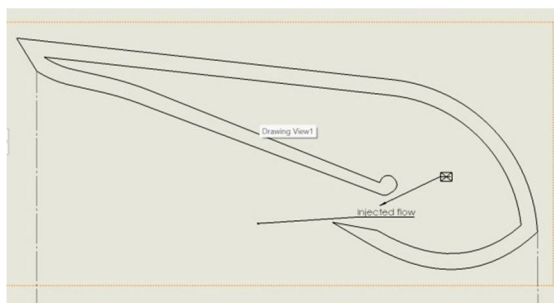


FIG 2. Coanda surface

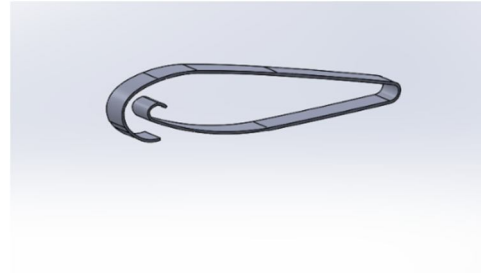
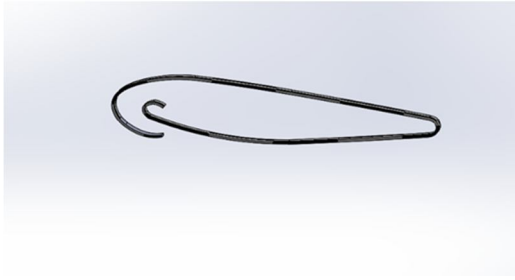
FIG 3. Entrainment air ejector surface is an axisymmetric device leveraging the injected outer curved surface. This device aims to achieve a high ratio of induced mass flow rate to injected mass flow rate, termed the "w factor." The primary flow, typically provided by a compressor, follows the curved contour of the ejector due to the Coanda effect, leading to the development of a turbulent mixing zone driven by expansion/compression waves at the outlet section. System performance in Coanda ejectors is influenced by factors such as pressure ratio, modifications possible to optimize thrust by adjusting parameters such as throat size, inlet duct length, hydraulic diameter, and taper angle. To achieve maximum thrust from each thruster, it's imperative to ensure a uniform, laminar flow of air along its thrust axis, free from any horizontal flow components inducing turbulence.

Another critical concept essential for successful thruster design is understanding the Coanda effect and its application in Coanda ejectors. The Coanda Surface, depicted in Figure 2, primary flow along the inward curved surface while entraining a secondary flow along the outlet and ejector configurations, and the growth of the mixing layer, crucial for enhancing the w factor and mixing length.

The velocity profile shape, as illustrated in Figure 2 and measured by the outlet throat gap, serves as an indicator of mixing characteristics. A flattened profile indicates complete mixing ratio between primary and secondary jets, essential for optimal ejector performance, ideally achieved closer to the inlet section to improve overall efficiency.

IV. DESIGN OF CROSS SECTION

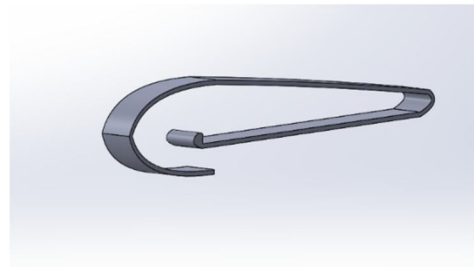
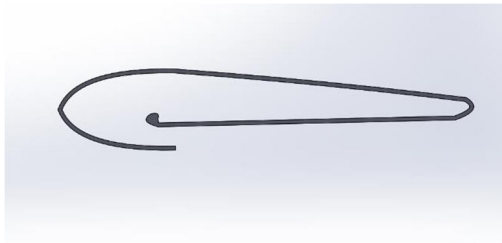
1) Design 1



2) Design 2



3) Design 3



The airfoil cross-section of the thruster undergoes meticulous design using SolidWorks, a renowned 3D CAD software. The selection of the optimal thruster design involves a comprehensive process, incorporating mass flow rate analysis and assessment of velocity differentials between the inlet and outlet. This evaluation is conducted through Ansys CFD, a sophisticated computational fluid dynamics tool. For the primary airfoil profile, the Eppler 473 profile is chosen due to its symmetric nature and its suitability as a Coanda surface. This profile facilitates proper curvature of airflow, ensuring efficient flow dynamics and enhancing the thruster's performance. Each design decision is carefully made to achieve optimal functionality and efficiency in the thruster's operation.

The process of selecting the most suitable thruster design involved a thorough Computational Fluid Dynamics (CFD) analysis. We opted for Ansys CFD software to conduct this analysis due to its reputation for accuracy and reliability in handling complex flow simulations. Ansys CFD allowed us to design and evaluate the cross-section of the thruster comprehensively.

In our study, we employed the k-epsilon turbulence model for the CFD analysis. This choice was based on its effectiveness in capturing turbulent flow phenomena, which are crucial considerations in aerodynamic applications such as thruster design. The k-epsilon model is well-regarded for its ability to predict turbulence effects accurately, making it a fitting selection for simulating the intricate flow dynamics around the thruster.

Using Ansys CFD provided several advantages for our analysis. It enabled us to develop a detailed computational model of the thruster's geometry, allowing for precise simulation of its aerodynamic behavior. Additionally, the software offered a range of post-processing tools for analyzing simulation results, facilitating comprehensive assessment and optimization of the thruster design.

V. RESULTS AND DISCUSSIONS

A. Analysis

For our study, we constructed a 76mm ducted fan operating at 4000 rpm. This led us to fix the inlet duct diameter at 76mm, while the maximum hydraulic diameter of the thruster outlet was determined to be 200mm.

To determine the mass flow rate required as an inlet boundary condition for our CFD analysis, we employed the following equations:

$$v = \frac{\pi ND}{60} \dots\dots\dots(1)$$

Where:

- v = is the velocity (m/s),
- N = is the rotational speed of the motor (rpm),
- D = is the diameter of the fan (m).

Substituting the given values into Equation (1):

$$v = \frac{3.14 \times 4000 \times 0.076}{60} = 16 \text{m/s}$$

Similarly,

The Mass flow rate m ,

$$m = \rho \left(\frac{\pi D^2}{4} \right) v \dots\dots\dots(2)$$

Where:

- m = is the mass flow rate (kg/s),
- ρ = is the density of air (1.225 kg/m³),
- A = is the area encompassed by the fan (m²).

$$= 1.225 \times (3.14 \times (0.076)^2 / 4) \times 16$$

$$= 0.088 \text{kg/s}$$

The summarized outcomes from the 3D flow examination of the three designs are presented in Table 1.

	Design 1	Design 2	Design 3
Inlet mass flow rate	0.08kg/s	0.08kg/s	0.08kg/s
Inlet velocity	16m/s	16m/s	16/s
Outlet mass flow rate	0.00020kg/s	0.061kg/s	0.0676kg/s
Velocity at outlet thrust	5.274m/s	4.6117m/s	27.175m/s
Thruster mass flow rate	0.1021kg/s	0.0841kg/s	0.29621kg/s

Table.1. results

Design 1 faced several limitations, notably the insignificantly small exit mass flow rate and the substantially reduced outlet velocity compared to the inlet velocity. Consequently, the thrust generated by this design was minimal.

Design 2, which aimed to enhance both the mass flow rate and outlet velocity by incorporating a convergent-divergent passage at the airfoil exit, encountered its own set of challenges. Although the mass flow rate approached that of the inlet, the outlet velocity remained significantly lower than desired.

However, Design 3 effectively addressed the shortcomings of both previous designs. With a throat size of 3mm (as illustrated in Fig.4(c)), Design 3 achieved a satisfactory level of thrust production. To facilitate a comprehensive comparison among the designs, various parameters were considered, the results of which are discussed in the subsequent section.

The consolidated outcomes of the 3D flow analysis for all three designs are presented in Table 1.

The subsequent parameter under consideration was the length of the inlet duct. Each design was experimented with two variants. In the first version, the inlet duct length was set at 30 mm, positioning the fan farther away from the thruster ring. In the second case, the fan was situated closer to the thruster ring, resulting in a shorter duct length of 10mm. Notably, it was observed that placing the duct closer to the ring resulted in a more evenly distributed flow at the exit of the thruster.

VI. MANUFACTURING

We determined that 3D printing offered the most suitable approach to validate our prototype. Through research and deliberation, it became evident that 3D printing was not only the fastest but also the most cost-effective method available. For this purpose, we utilized PLA (Poly Lactic Acid) as the printing material as it is cost effective and well Suited for the prototype we expect . Subsequently, the prototype was employed to verify the simulated results. The weight of the model was measured at 250g. The prototype used for validation is depicted in Fig. 6.



Fig.6

VII. LITERATURE REVIEW

The evolution of unmanned aerial vehicles (UAVs) has seen a shift towards innovative propulsion systems, departing from traditional propeller-based designs. Bladeless fan technology, a notable advancement in aerodynamics, has garnered attention for its potential applications in UAVs, particularly quadcopters. This literature review delves into the realm of bladeless fan technology and its integration into quadcopter design and analysis.

Emerging from companies like Dyson, bladeless fan technology operates on principles distinct from conventional propellers. Its operation relies on the Coanda effect and inducement, drawing in air through a ring-shaped structure to create a powerful stream. This technology offers several benefits, including reduced noise emissions, enhanced safety, and the prospect of heightened efficiency compared to traditional propeller systems.

The utilization of bladeless fan technology in quadcopter propulsion opens new avenues and challenges. Previous studies have explored the feasibility of employing bladeless fans for lift and maneuverability in UAVs. For instance, Li et al. (2020) conducted experiments showcasing a prototype quadcopter equipped with bladeless fans, demonstrating its ability to achieve stable flight and generate lift. Their findings underscored potential advantages such as improved safety and decreased noise pollution, especially in urban settings.

Designing a quadcopter driven by bladeless fans necessitates considerations spanning aerodynamic efficiency, power consumption, stability, and control mechanisms. Researchers have focused on optimizing the design and configuration of bladeless fan units to maximize thrust while minimizing energy requirements. Computational fluid dynamics (CFD) simulations have played a crucial role in analyzing airflow patterns and refining bladeless fan designs for UAV applications.

Performance evaluation of bladeless fan- powered quadcopters encompasses metrics such as lift capacity, maneuverability, endurance, and noise levels. Comparative studies between traditional propeller-driven quadcopters and bladeless fan quadcopters have provided insights into the advantages and limitations of each propulsion system. These studies contribute valuable knowledge regarding operational capabilities and potential trade-offs associated with adopting bladeless fan technology in UAVs.

While current research demonstrates the feasibility and benefits of bladeless fan technology in quadcopter applications, numerous avenues for future exploration

exist. These include further refinement of bladeless fan designs, integration of advanced control algorithms for enhanced stability and agility, exploration of hybrid propulsion systems combining bladeless fans with other technologies, and real- world testing under diverse environmental conditions.

In conclusion, bladeless fan technology presents an intriguing alternative for propulsion and control in quadcopters, offering potential advantages in terms of safety, noise reduction, and aerodynamic efficiency. Continued research and development efforts in this domain are crucial to fully harnessing the capabilities of bladeless fan-powered UAVs and expanding their applications across various industries.

The evolution of propulsion technologies has seen a significant transformation with the advent of bladeless thrusters. Traditional propulsion systems, which rely on propellers or turbines, are being reimagined through bladeless designs. This literature review aims to provide an overview of the current research and advancements in bladeless thrusters, focusing on their design, development, and performance analysis.

Bladeless thrusters, inspired by innovations such as the Dyson Air Multiplier, operate on principles distinct from conventional propellers. They leverage the Coanda effect and air induction to create a continuous airflow without exposed blades. This technology offers several benefits including reduced noise, increased safety, and potentially higher efficiency. The absence of external blades mitigates the risk of mechanical failure and injury, making these thrusters particularly appealing for various applications. Designing a bladeless thruster involves complex aerodynamic considerations. Researchers have focused on optimizing the geometry of the thruster to maximize airflow and thrust while minimizing power consumption. Key design parameters include the shape of the airfoil, the size of the air intake, and the configuration of the internal channels. Studies, such as those conducted by Gupta et al. (2019), have utilized computational fluid dynamics (CFD) simulations to refine these parameters and achieve optimal performance. Performance analysis of bladeless thrusters encompasses evaluating thrust generation, energy efficiency, and acoustic properties. Comparative studies have been conducted to benchmark the performance of bladeless thrusters against traditional propeller-based systems. For instance, experiments by Li et al. (2020) demonstrated that bladeless thrusters could achieve comparable thrust levels with significantly reduced noise output. These findings suggest that bladeless thrusters are not only quieter but also more suitable for applications requiring low acoustic signatures, such as surveillance and urban air mobility.

One of the most promising applications of bladeless thrusters is in unmanned aerial vehicles (UAVs). The integration of bladeless technology in UAVs offers numerous advantages, including improved safety, reduced maintenance requirements, and enhanced aerodynamic efficiency. Research by Sunil Kumar et al. (2021) explored the feasibility of using bladeless thrusters in quadcopters, highlighting their potential to enhance flight stability and control precision. The absence of rotating blades reduces the risk of damage during collisions, making bladeless thrusters ideal for UAVs operating in cluttered or confined environments. Despite their advantages, bladeless thrusters face several challenges.

The primary challenge lies in achieving sufficient thrust and efficiency to compete with traditional systems. Ongoing research is focused on improving the aerodynamic design and material efficiency to enhance performance. Future research directions include the development of hybrid systems that combine bladeless thrusters with conventional propulsion methods, advanced control algorithms for improved stability, and extensive real-world testing under various conditions to validate their performance and reliability. Bladeless thruster technology represents a significant advancement in propulsion systems, offering unique benefits in terms of safety, noise reduction, and efficiency. While challenges remain, particularly in achieving optimal thrust and efficiency, ongoing research and development efforts continue to push the boundaries of what these systems can achieve. The integration of bladeless thrusters in UAVs and other applications holds great promise, potentially revolutionizing the way we approach aerial and marine propulsion.

VIII. CONCLUSION

This paper presents the design and implementation of a bladeless propulsion system that has potential applications in unmanned aerial vehicles (UAVs). The system features a ducted fan or compressor and an outlet frame with an inlet that creates a suction effect, entraining ambient air. The resulting pressure difference, along with the Coanda effect, is fundamental for generating thrust. The design process involved selecting an optimal airfoil for the engine's cross-section and using computational fluid dynamics (CFD) analysis to evaluate and optimize the design. Out of the three engine designs considered, Design 3 provided the best thrust performance.

The findings suggest that the bladeless propulsion system has the potential to improve the efficiency and performance of UAVs compared to conventional propulsion systems. The successful validation of the prototype through 3D printing indicates the feasibility of this innovative approach.

REFERENCES

- [1] Luis Rodolfo Garcia Carrillo , Pablo Rangel 2018, Improving Safety: Design and Development of a Bladeless Thruster for Autonomous Multicopters, DOI: 10.1109/ICUAS.2018.8453474
- [2] Ruixiong Li, Huanran Wang, Erren Yao, Meng Li and Weigang Nan, 2017, Experimental study on bladeless turbine using incompressible working medium, DOI: 10.1177/1687814016686935
- [3] M. Jafari, H. Afshin † , B. Farhanieh and H. Bozorgasareh, Numerical Aerodynamic Evaluation and Noise Investigation of a Bladeless Fan - Journal of Applied Fluid Mechanics, Vol. 8, No. 1, pp. 133-142, 2015.



- [4] Li, G., & Hu, Y., & Jin, Y., & Setoguchi, T., & Kim, H. D. (2014). Influence of Coanda surface curvature on performance of bladeless fan. *Journal of thermal science*, 23(5), 422-431. <https://doi.org/10.1007/s11630-014-0725-3>
- [5] Darvishpoor, S., & Roshanian, J., & Raissi, A., & Hassanalian, M. (2020). Configurations, flight mechanisms, and applications of unmanned aerial systems: A review. *Progress in Aerospace Sciences*, 121, 100694
- [6] T. Benson, "General Thrust Equation", NASA, NASA, 12 June 2014, spaceflightssystemsgrc.nasa.gov/education/rocket/thrsteq.html
- [7] Lasse C. M ansson, Simon H. Traberg-Larsen, 2014, Flow Characteristics of the Dyson Air Multiplier



10.22214/IJRASET



45.98



IMPACT FACTOR:
7.129



IMPACT FACTOR:
7.429



INTERNATIONAL JOURNAL FOR RESEARCH

IN APPLIED SCIENCE & ENGINEERING TECHNOLOGY

Call : 08813907089  (24*7 Support on Whatsapp)